2.2.3. Delft3D-MOR

The module Delft3D-MOR combines the information provided by the flow and wave modules to compute the sediment transport fluxes. The seabed level can then be updated as a result of the sediment sink and sources terms and computed transport gradients.

The updated expressions of Van Rijn, known as TRANSPOR2004 (Van Rijn, et al., 2004; Van Rijn, 2007a; Van Rijn, 2007b) were used to calculate the total sediment transport, including the bed load transport q_b and the suspended load transport q_s.

The bed load transport component consists of a current-related contribution (in the current direction), and a wave-related contribution (in the wave direction, following or opposing, depending on conditions). The suspended load transport includes a current-related contribution, due to advective processes (in the current direction) and the wave-related contribution, (in the wave direction, always onshore). Both wave contributions account for the wave asymmetry effects that develop as waves propagate in shallow waters due to non-linear processes.

The computation of the bed-load transport is based on the concept of the instantaneous bed-shear stress. The instantaneous bed-load transport rate $q_{b,t}$ is related to the instantaneous bed-shear stress, which is based on the instantaneous velocity vector (including both wave-related and current-related components; numerical intrawave approach) defined at the top of the bed load layer (i.e. small height above seabed) (Van Rijn, 2007 a). The oscillating wave-induced near bed orbital velocity due to asymmetry effects is modelled using the method of Isobe–Horikawa (1982) modified by Grasmeijer (2002).

The instantaneous bed load transport is computed as follows:

$$q_{b,t} = 0.5\,.\,\rho_s\,.\,d50\,.\,D_*^{-0.3}\,.\left(\frac{\tau_{b,cw,t}}{\rho}\right)^{0.5}\left(\frac{\max(0,\tau_{b,cw,t}-\tau_{b,cr})}{\tau_{b,cr}}\right) \qquad (2.1)$$

in which ρ_s is the sediment volumic mass, d50 is median grain size, D* is the dimensionless particle size, ρ is water volumic mass, $\tau_{b,cw,t}$ is the instantaneous bed shear stress due to combined wave and current action and $\tau_{b,cr}$ the critical bed shear stress according to Shields.

The net bedload transport vector is obtained by time-averaging of the instantaneous bed-load transport vector over a wave period T.

$$q_b = \frac{1}{T}\int q_{b,t}\;.dt \qquad (2.2)$$

Furthermore, the magnitude and direction of the bed load transport vector can be adjusted for bed slope effects.

The current-related suspended load transport consists in the transport of sediment particles by the time-averaged current velocities. It is calculated as the product of the velocity profile and the concentration profile, obtained by solving the advection-diffusion equation (Van Rijn, 2007 b) :

$$q_{s,c} = \int_a^h u\,.\,c\,.\,dz \qquad (2.3)$$

Hs=3m, Dir=135 deg., Tp=14 s. **Hs=3m, Dir=45 deg., Tp=10 s.**

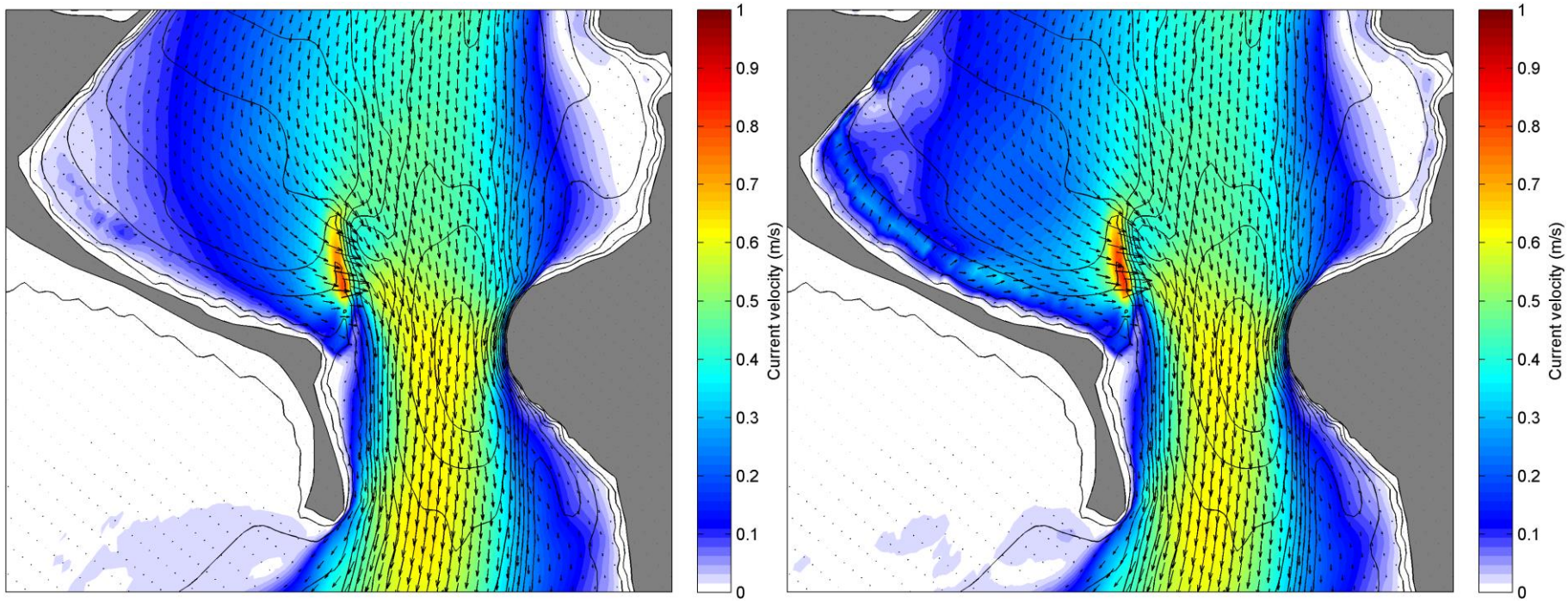

Figure 3.12 Mean flow fields within the entrance region for incoming tide phases, for high energy southeast (left) and northeast (right) wave events (southeast event: Hs=3m, Dir=135 deg., Tp=14 s.; northeast event: Hs=3m, Dir=45 deg., Tp=10 s.)

Hs=3m, Dir=135 deg., Tp=14 s.

Hs=3m, Dir=45 deg., Tp=10 s.

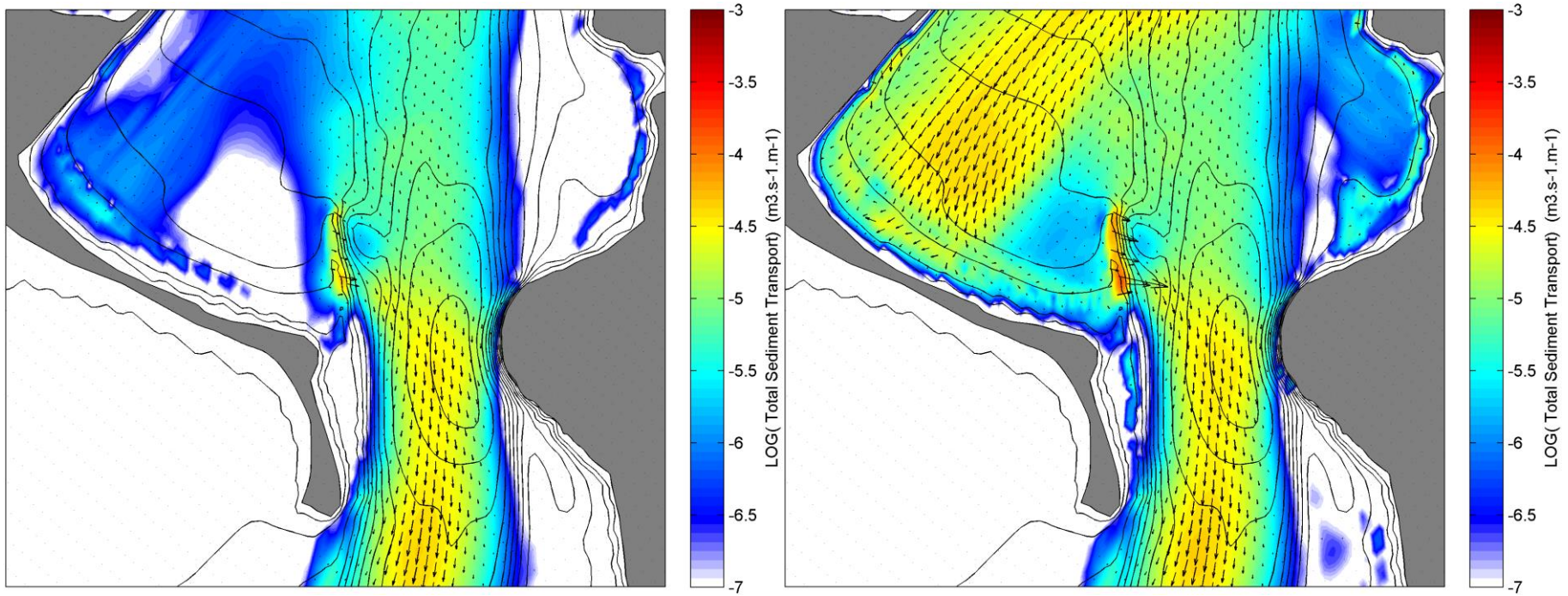

Figure 3.13 Mean total sediment transport fluxes within the entrance region for incoming tide phases, for high energy southeast (left) and northeast (right) wave events (southeast event: Hs=3m, Dir=135 deg., Tp=14 s.; northeast event: Hs=3m, Dir=45 deg., Tp=10 s.)

Hs=2m, Dir=0 deg., Tp=14 s. **Hs=1m, Dir=0 deg., Tp=8 s.**

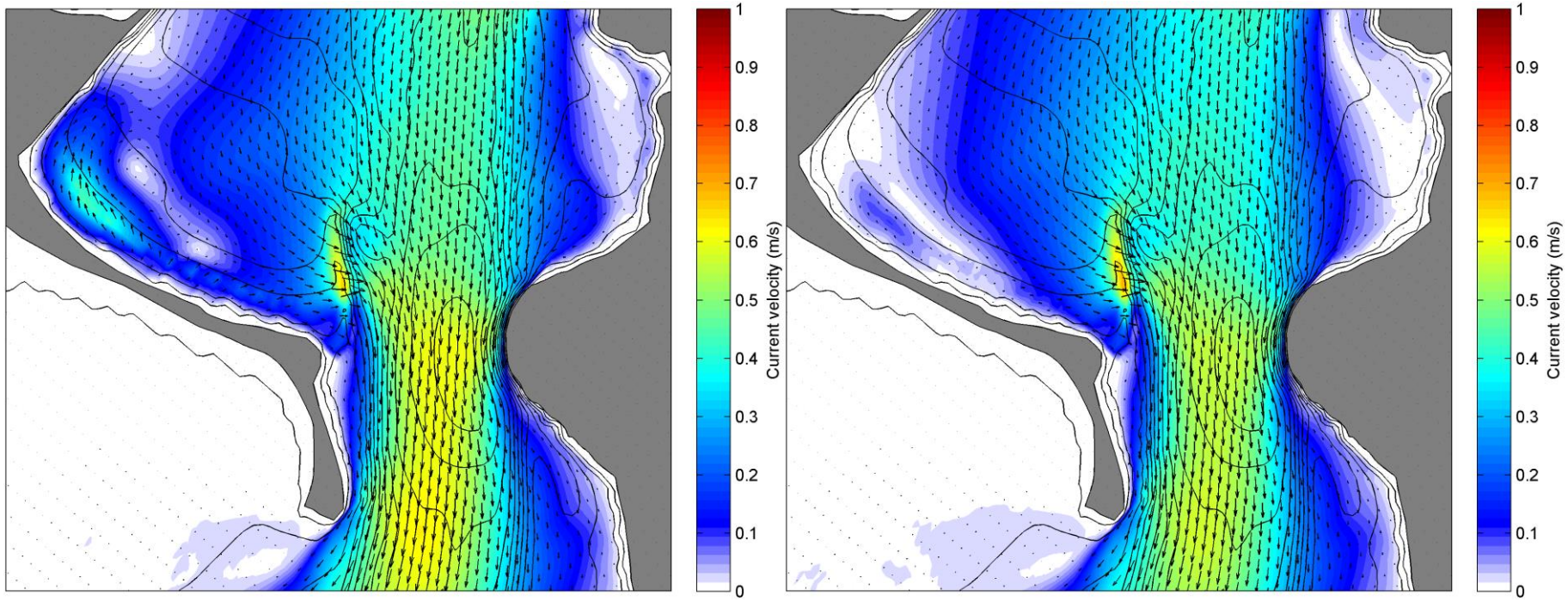

Figure 3.14 Mean flow fields within the entrance region for incoming tide phases, for high energy north swell waves (left) and low energy sea waves (north swell event: Hs=2m, Dir=0 deg., Tp=14 s.; north sea event: Hs=1m, Dir=0 deg., Tp=8 s.)

Hs=2m, Dir=0 deg., Tp=14 s.

Hs=1m, Dir=0 deg., Tp=8 s.

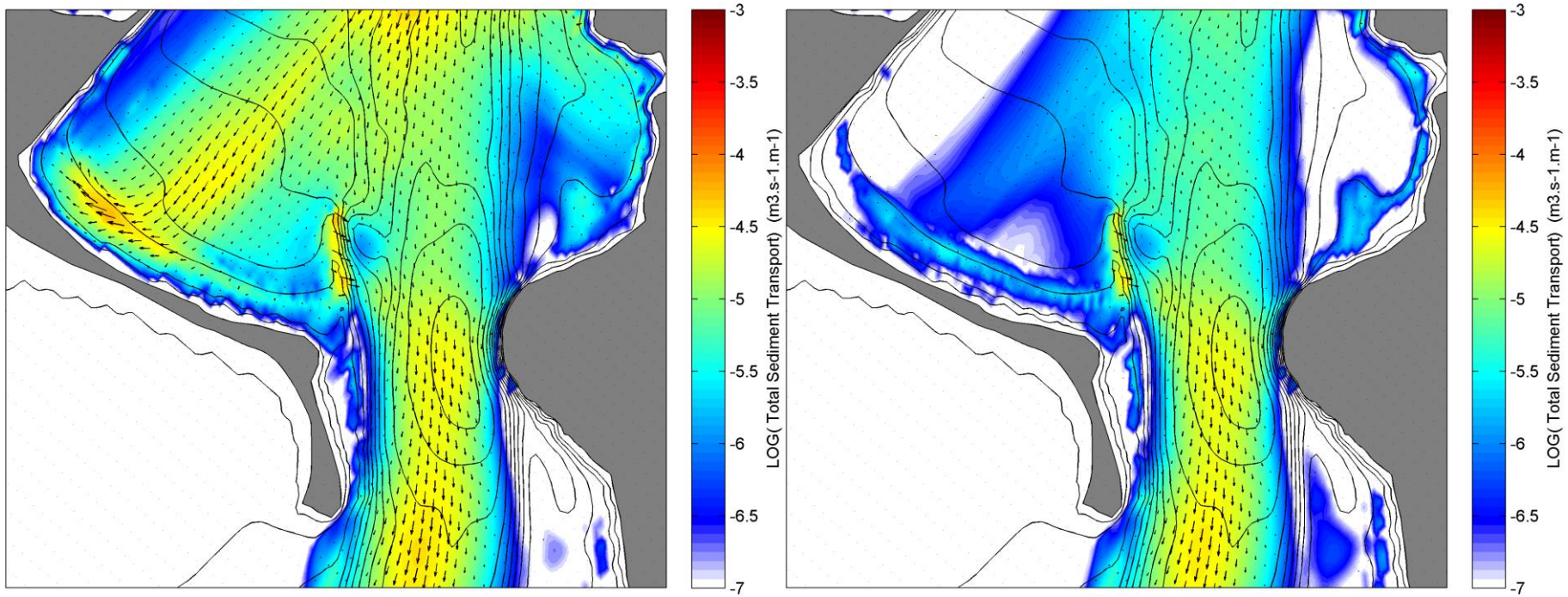

Figure 3.15 Mean total sediment transport fluxes within the entrance region for incoming tide phases, for high energy north swell waves (left) and low energy sea waves. (north swell event: Hs=2m, Dir=0 deg., Tp=14 s.; north sea event: Hs=1m, Dir=0 deg., Tp=8 s.)

Hs=3m, Dir=135 deg., Tp=14 s. **Hs=3m, Dir=45 deg., Tp=10 s.**

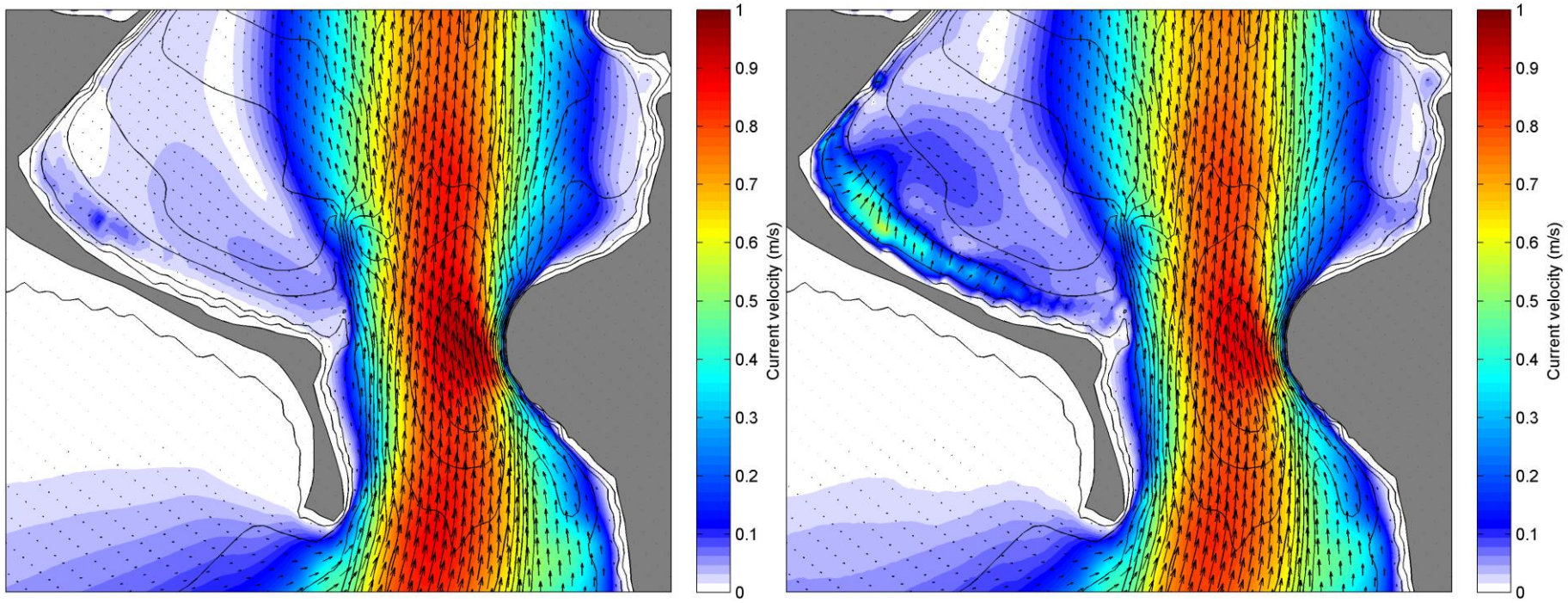

Figure 3.16 Mean flow fields within the entrance region for outgoing tide phases, for high energy southeast (left) and northeast (right) wave events (southeast event: Hs=3m, Dir=135 deg., Tp=14 s.; northeast event: Hs=3m, Dir=45 deg., Tp=10 s.)

Hs=3m, Dir=135 deg., Tp=14 s. **Hs=3m, Dir=45 deg., Tp=10 s.**

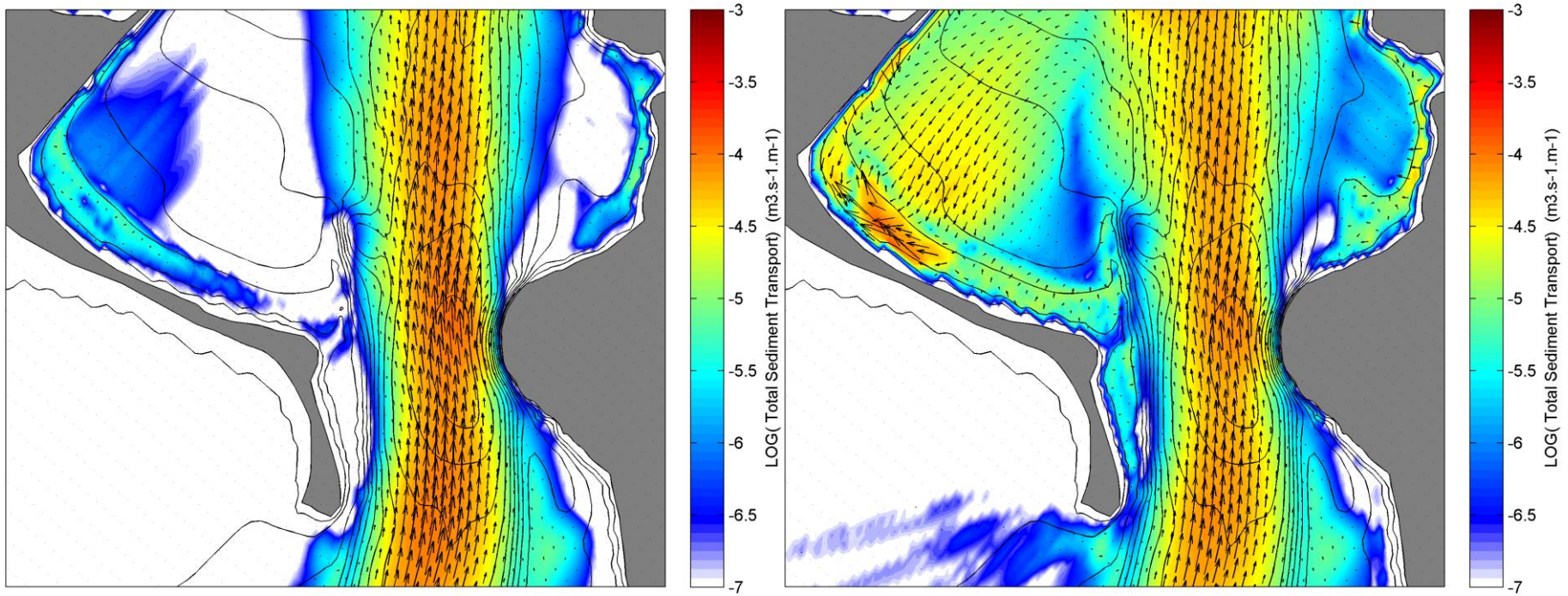

Figure 3.17 Mean total sediment transport fluxes within the entrance region for outgoing tide phases, for high energy southeast (left) and northeast (right) wave events (southeast event: Hs=3m, Dir=135 deg., Tp=14 s.; northeast event: Hs=3m, Dir=45 deg., Tp=10 s.)

Hs=2m, Dir=0 deg., Tp=14 s.

Hs=1m, Dir=0 deg., Tp=8 s.

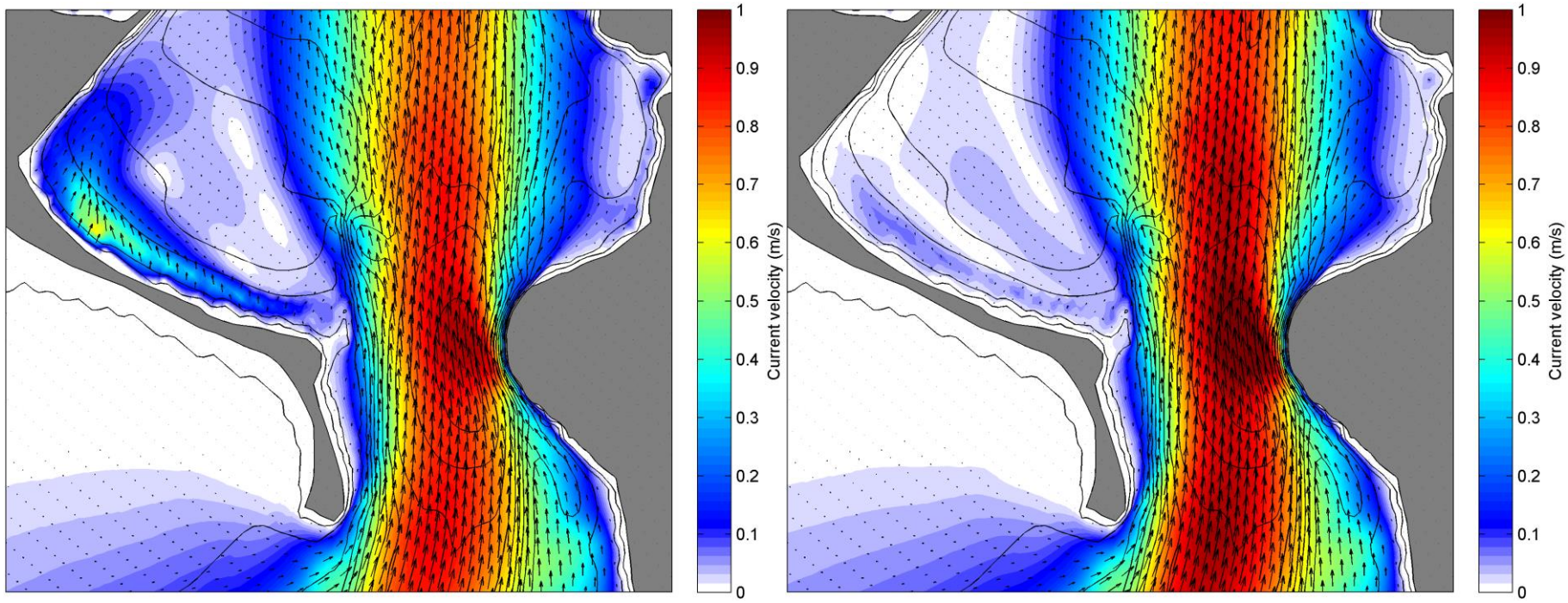

Figure 3.18 Mean flow fields within the entrance region for outgoing tide phases, for high energy north swell waves (left) and low energy sea waves (north swell event: Hs=2m, Dir=0 deg., Tp=14 s.; north sea event: Hs=1m, Dir=0 deg., Tp=8 s.)

Hs=2m, Dir=0 deg., Tp=14 s.

Hs=1m, Dir=0 deg., Tp=8 s.

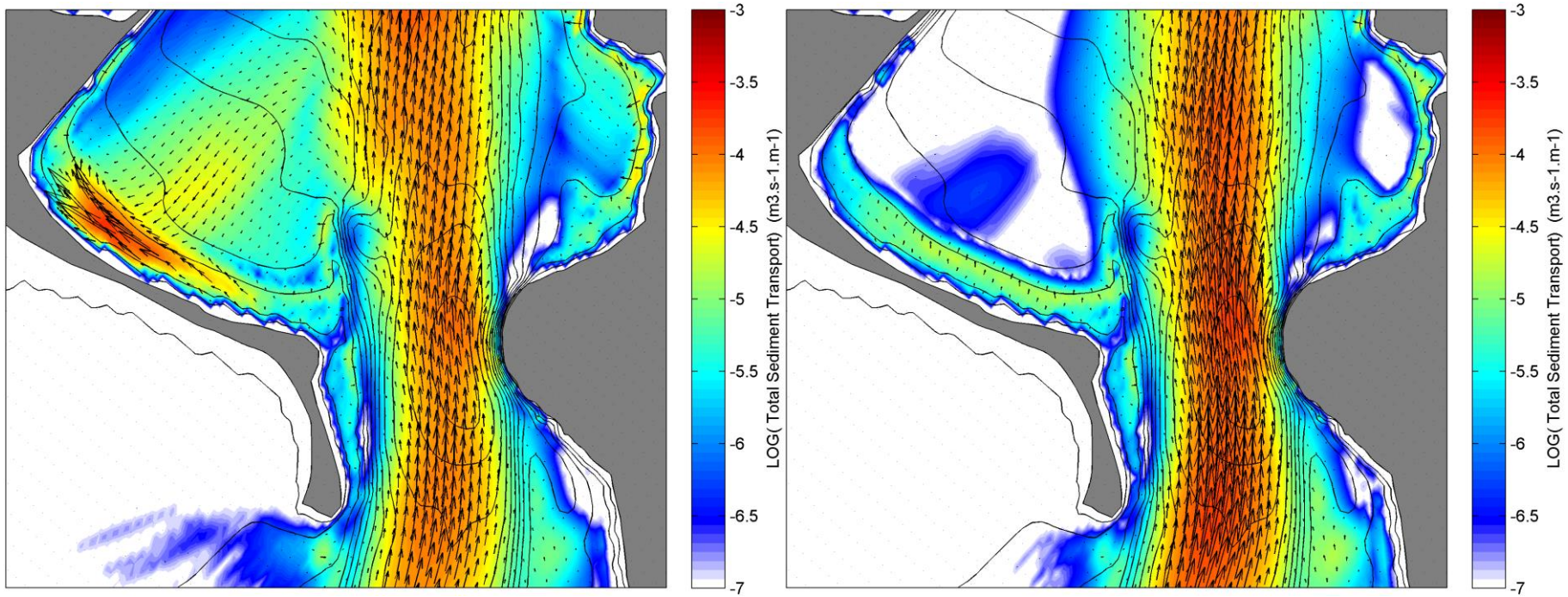

Figure 3.19 Mean total sediment transport fluxes within the entrance region for outgoing tide phases, for high energy north swell waves (left) and low energy sea waves. (north swell event: Hs=2m, Dir=0 deg., Tp=14 s.; north sea event: Hs=1m, Dir=0 deg., Tp=8 s.)

Hs=3m, Dir=135 deg., Tp=14 s. **Hs=3m, Dir=45 deg., Tp=10 s.**

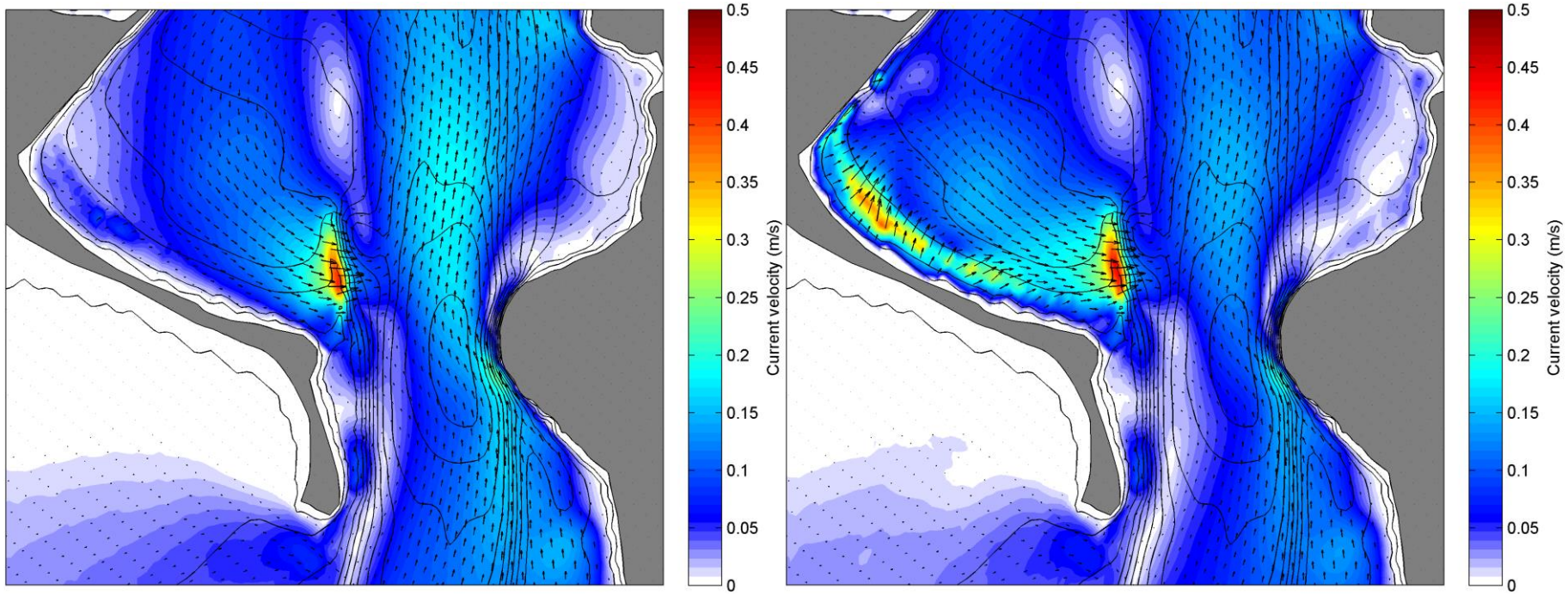

Figure 3.20 Mean flow fields within the entrance region for the full tidal cycles, for high energy southeast (left) and northeast (right) wave events (southeast event: Hs=3m, Dir=135 deg., Tp=14 s.; northeast event: Hs=3m, Dir=45 deg., Tp=10 s.)

Hs=3m, Dir=135 deg., Tp=14 s. **Hs=3m, Dir=45 deg., Tp=10 s.**

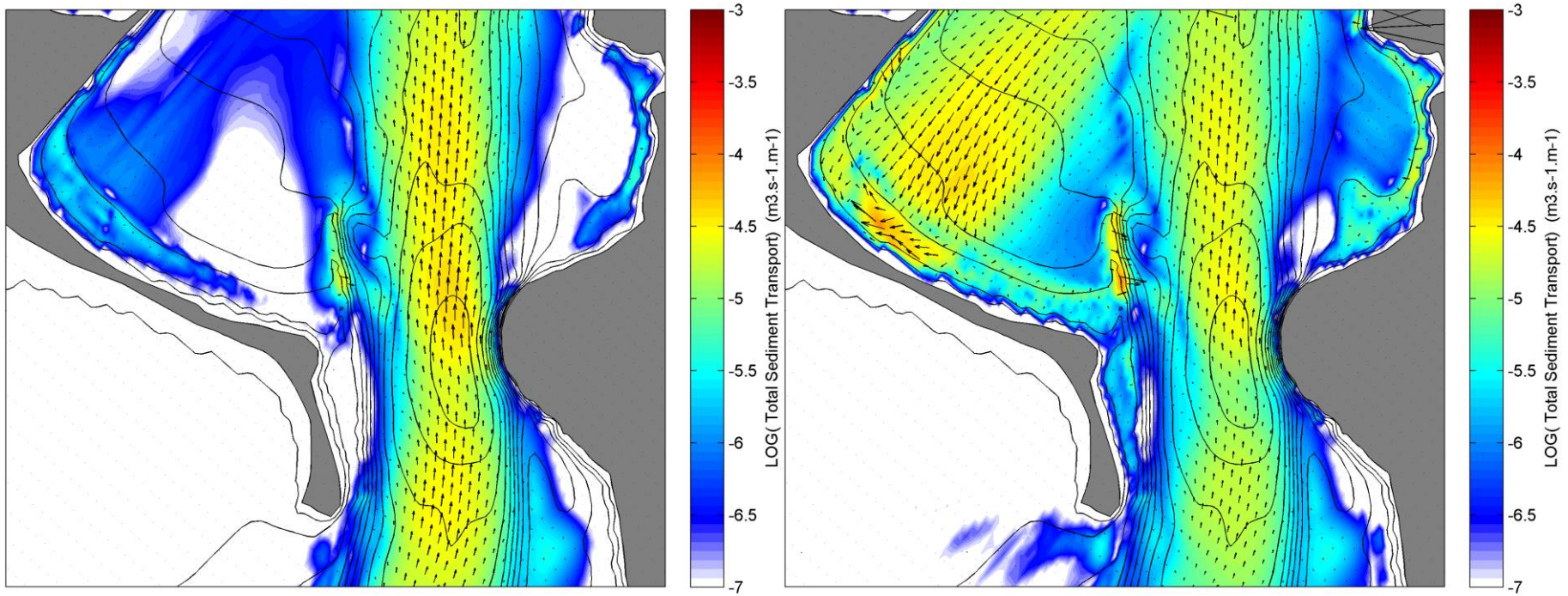

Figure 3.21 Mean total sediment transport fluxes within the entrance region for the full tidal cycles, for high energy southeast (left) and northeast (right) wave events (southeast event: Hs=3m, Dir=135 deg., Tp=14 s.; northeast event: Hs=3m, Dir=45 deg., Tp=10 s.)

Hs=2m, Dir=0 deg., Tp=14 s.

Hs=1m, Dir=0 deg., Tp=8 s.

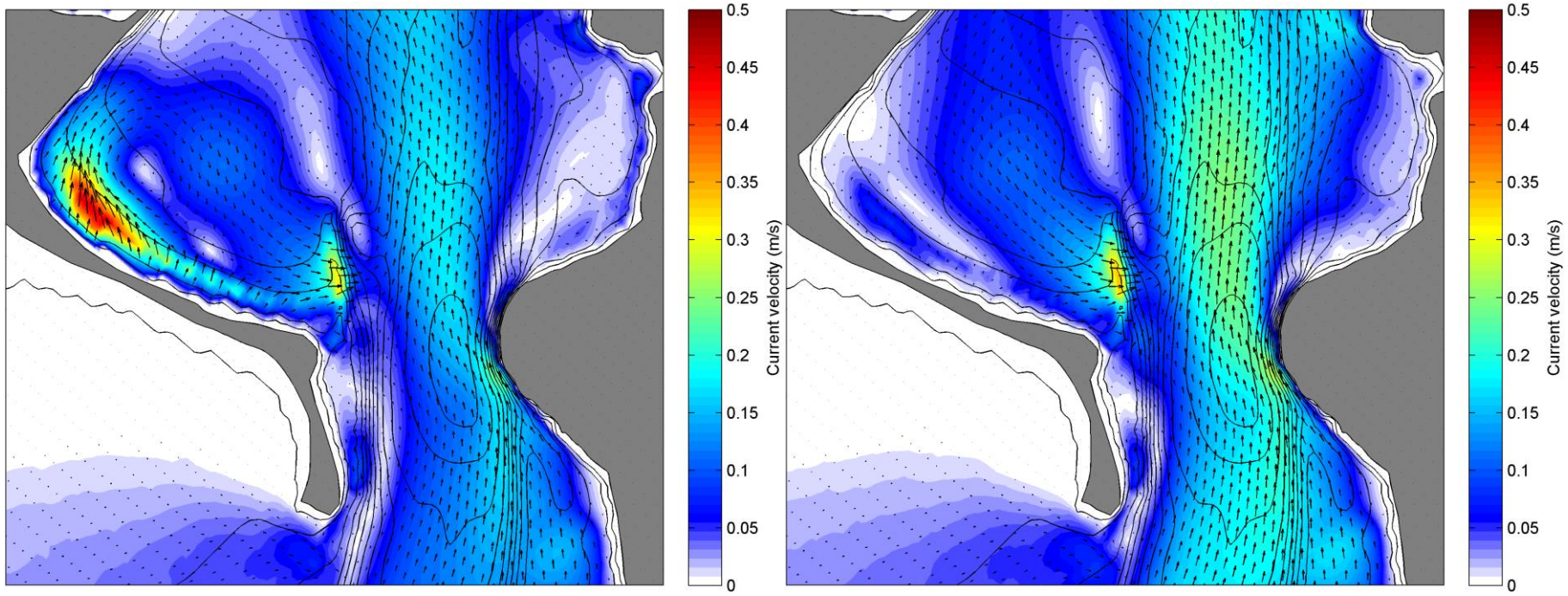

Figure 3.22 Mean flow fields within the entrance region for the full tidal cycles, for high energy north swell waves (left) and low energy sea waves (north swell event: Hs=2m, Dir=0 deg., Tp=14 s.; north sea event: Hs=1m, Dir=0 deg., Tp=8 s.)

Hs=2m, Dir=0 deg., Tp=14 s.

Hs=1m, Dir=0 deg., Tp=8 s.

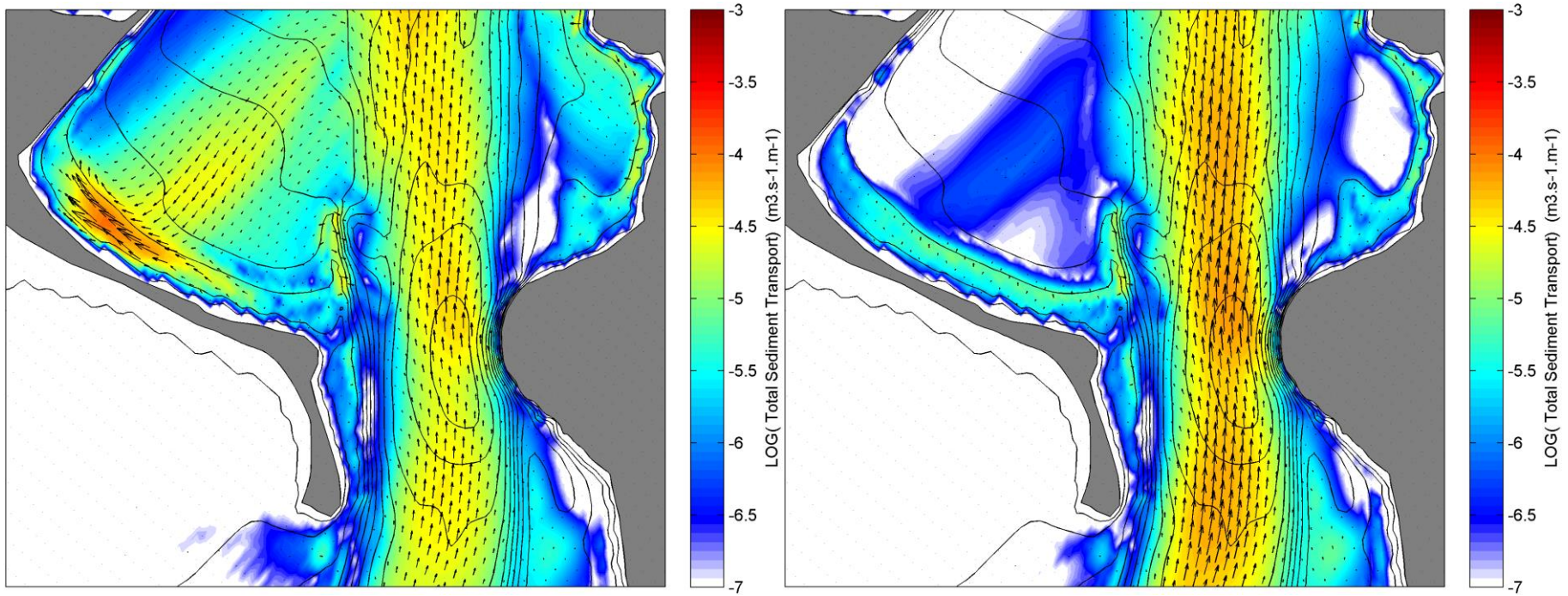

Figure 3.23 Mean total sediment transport fluxes within the entrance region for the full tidal cycles, for high energy north swell waves (left) and low energy sea waves. (north swell event: Hs=2m, Dir=0 deg., Tp=14 s.; north sea event: Hs=1m, Dir=0 deg., Tp=8 s.)

Incoming tides **Outgoing tides**

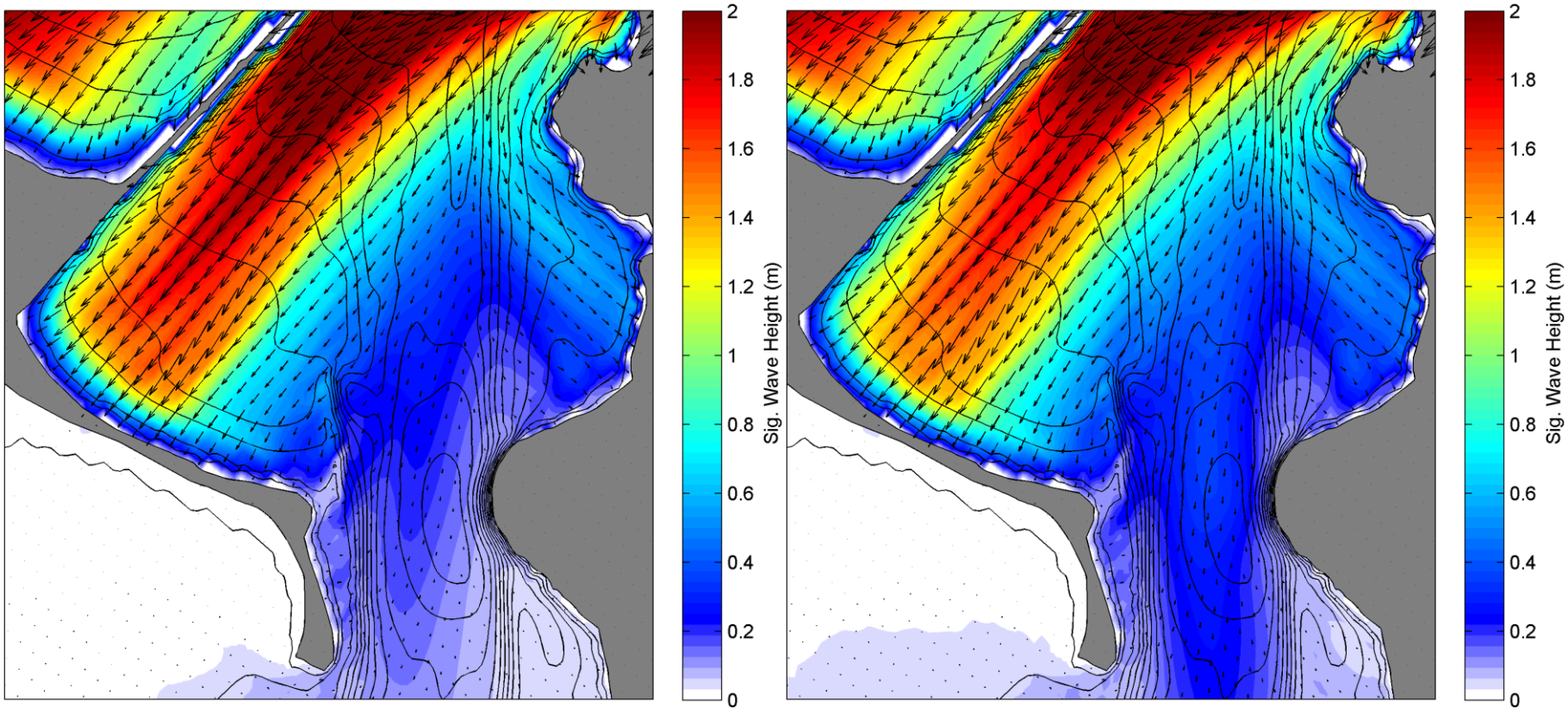

Figure 3.24 Mean significant wave heights at incoming and outgoing tide phases for the high energy northeast event (Hs=3m, Dir=45 deg., Tp=10 s.)

Incoming tides **Outgoing tides**

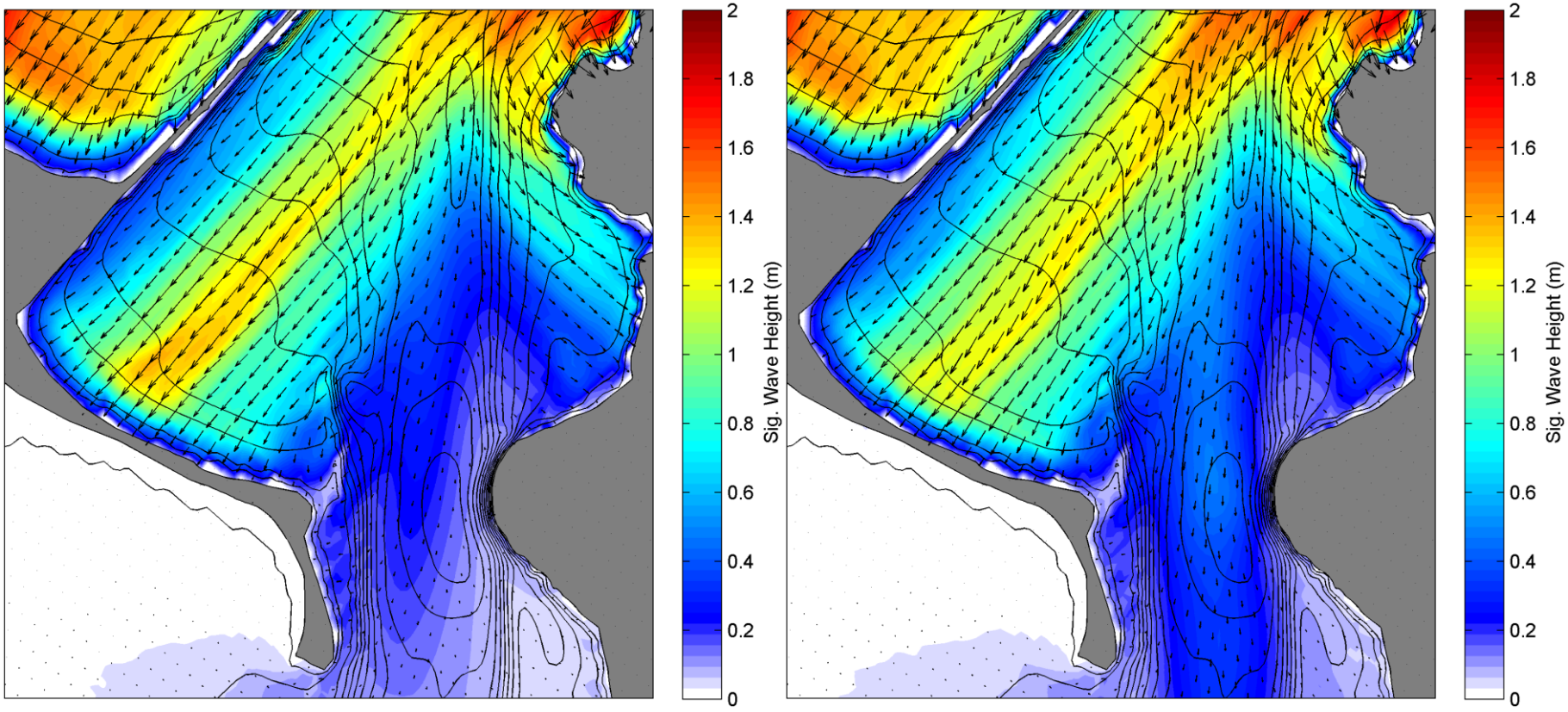

Figure 3.25 Mean significant wave heights at incoming and outgoing tide phases for the high energy north swell event (Hs=2m, Dir=0 deg., Tp=14 s).

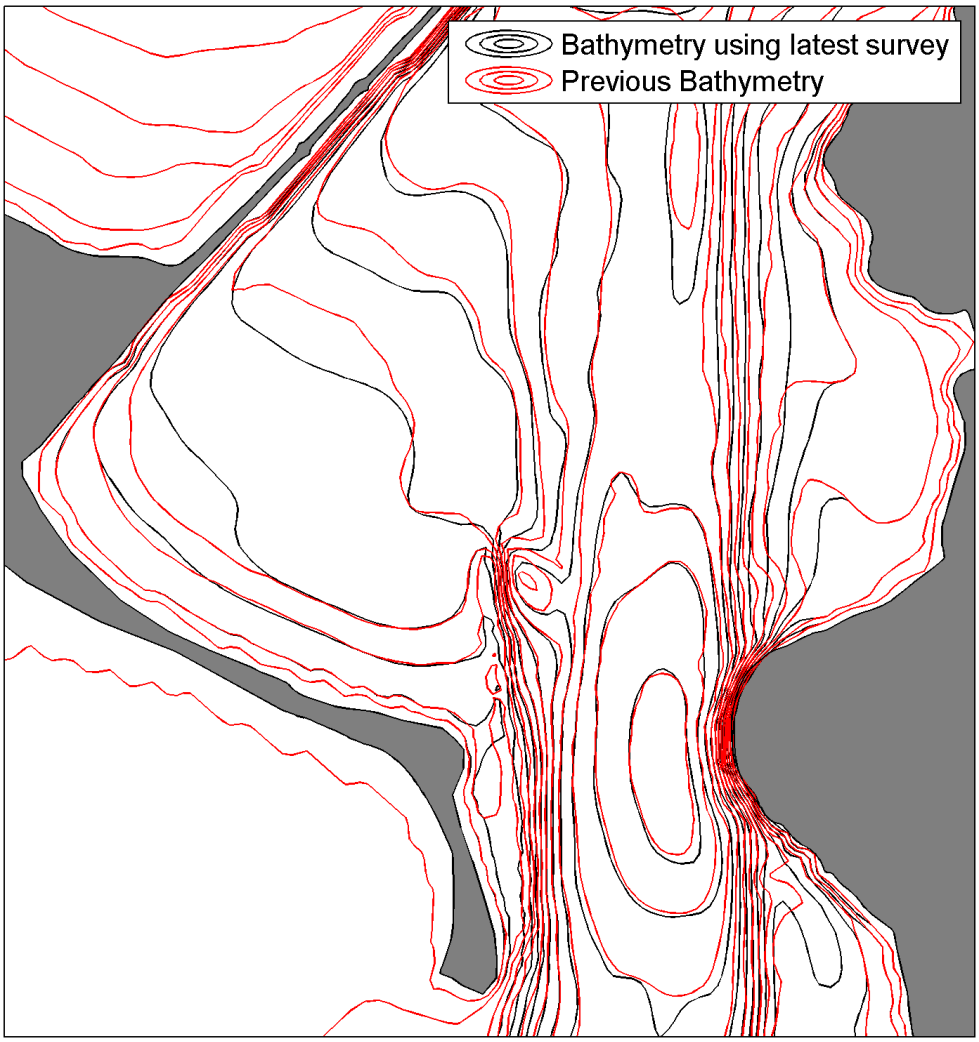

Figure 3.26 Depth contours of previous bathymetry (red) and bathymetry including the latest survey from the entrance region (black). Note the onshore translation of contours coinciding with the wave penetration zones in Figures 3.10 and 3.11.

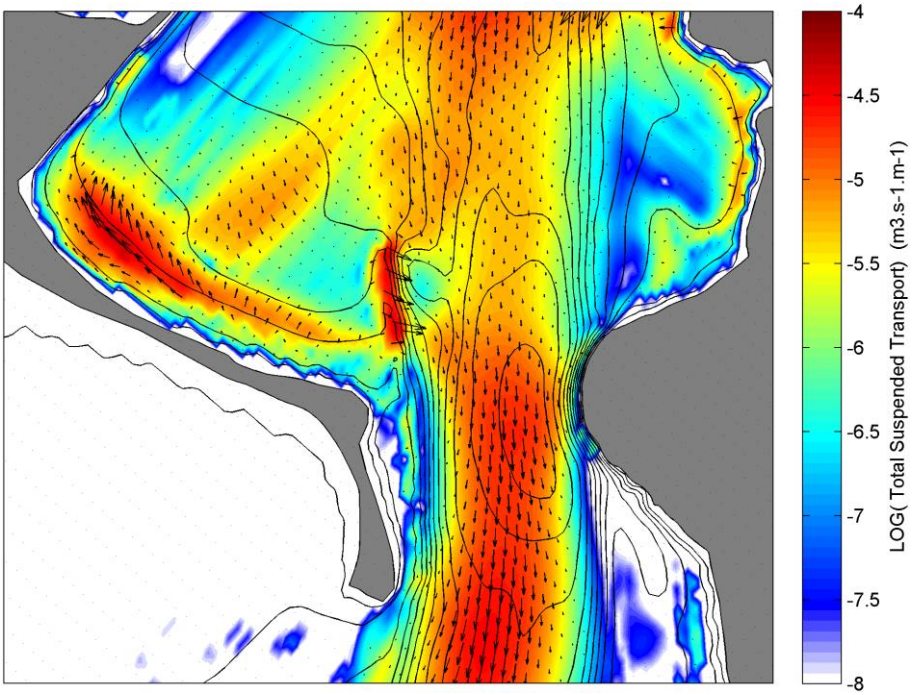

Figure 3.27 Mean suspended sediment transport fluxes within the entrance region for the full tidal cycles, for the high energy north swell event (Hs=2m, Dir=0 deg, T=14 s.). Note the different color scale relative to total transport maps.

4. LONG MAC OPTIMISATION RESULTS

4.1. Bathymetry modifications

The implemented numerical model provides a tool to test the efficacy of different structure configurations to reduce sediment recirculation into the Harbour. Based on the previous findings, incoming tides are of particular interest since the ambient tidal dynamics and wave-driven forces will work in combination to drive strong longshore flows and transport fluxes over the existing structure and into the channel. In that sense an option could be to try to physically block this longhsore transport feature by keeping the existing structure position but raising its crest.

Net flow and transport patterns during incoming tides clearly indicate that the central part of the existing structure, just west of the existing beach/spit bend is a critical spot with respect to sediment transport (see Figures 3.9 and 3.11 to 3.14). The existing structure was split into three segments of similar lengths. Two scenarios were considered, one in which only the central part is raised, and another in which the central and north sections are raised, thus providing a more significant blocking of the flow. In both cases, the structure level in the model was raised to +1.1 m relative to mean sea level which is the predicted highest astronomical tide (HAT) so that the structure is emergent at all tidal stages. Note that in addition to raising the structure in its longitudinal axis (i.e. approximately North-South), the junction to the existing beach (i.e. in the vicinity of the existing groin) is raised to a similar level so that the Shelly Beach cell is enclosed. A definition sketch of the segments considered is shown in Figure 4.1 and the existing bathymetry and configurations with emerged segments are shown in Figure 4.2. Bed level differences between the modified and existing bathymetries are shown in Figure 4.3 for both configurations.

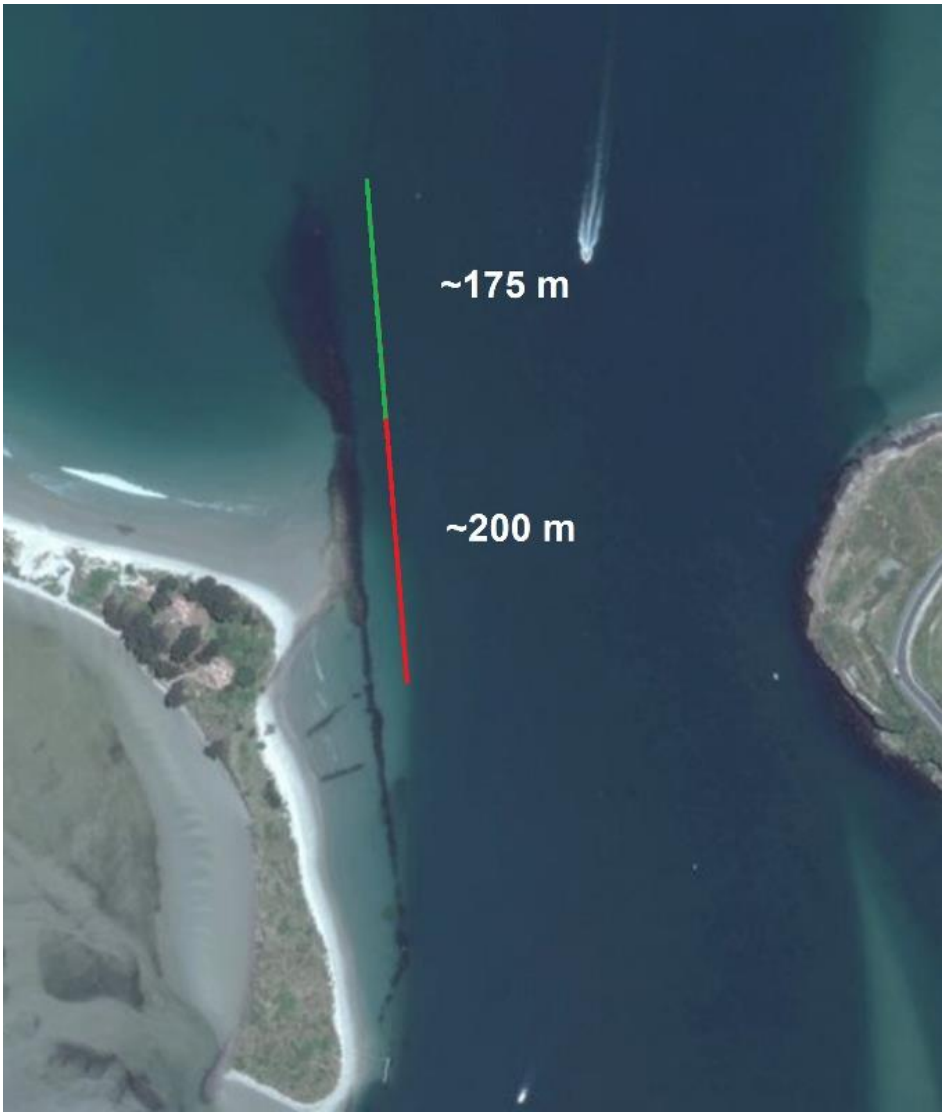

Figure 4.1 Aerial view of the Long Mac structure with definition of segments raised to +1.1 m MSL (highest astronomical tide).

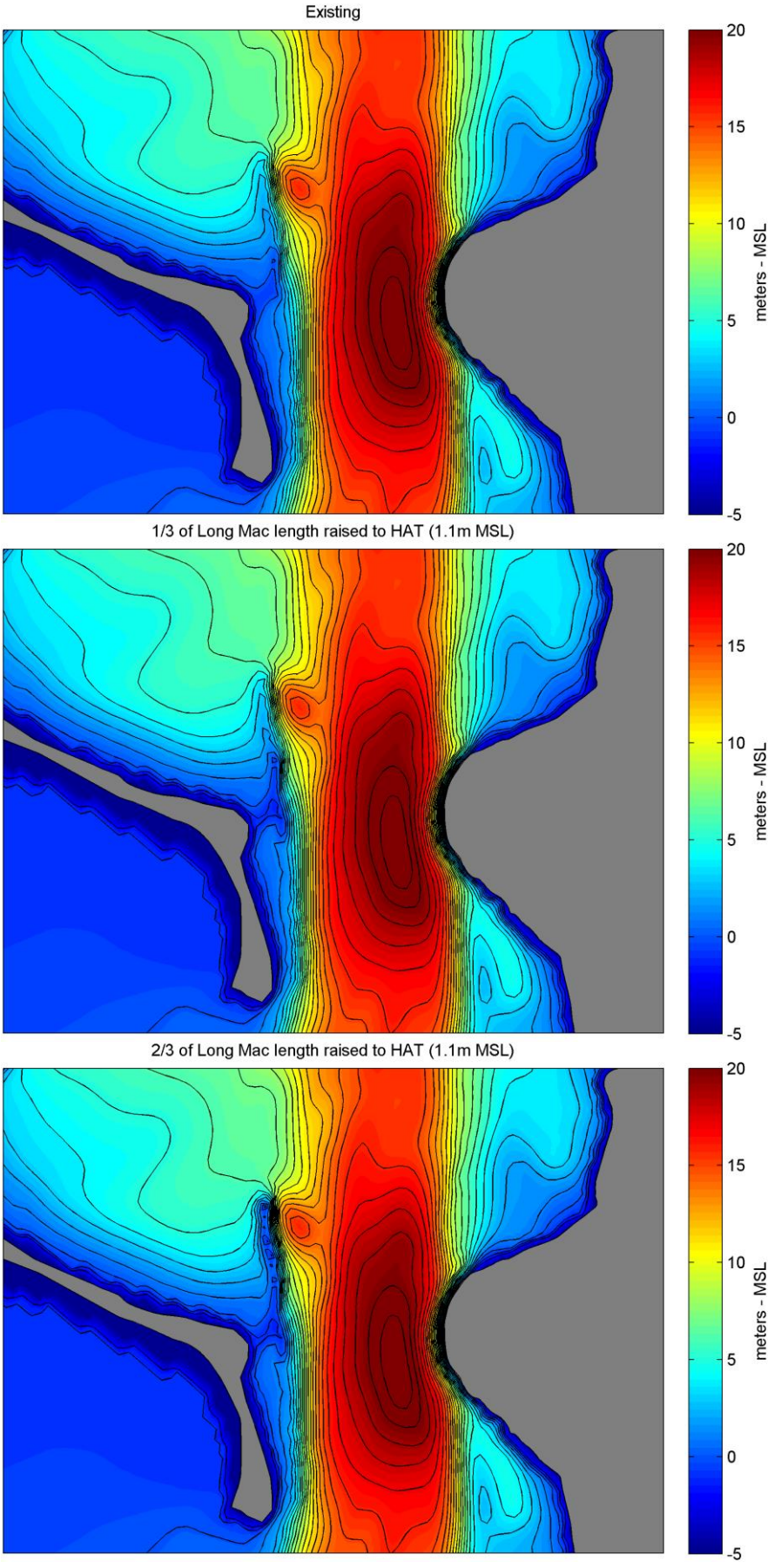

Figure 4.2. Existing and modified model bathymetries.

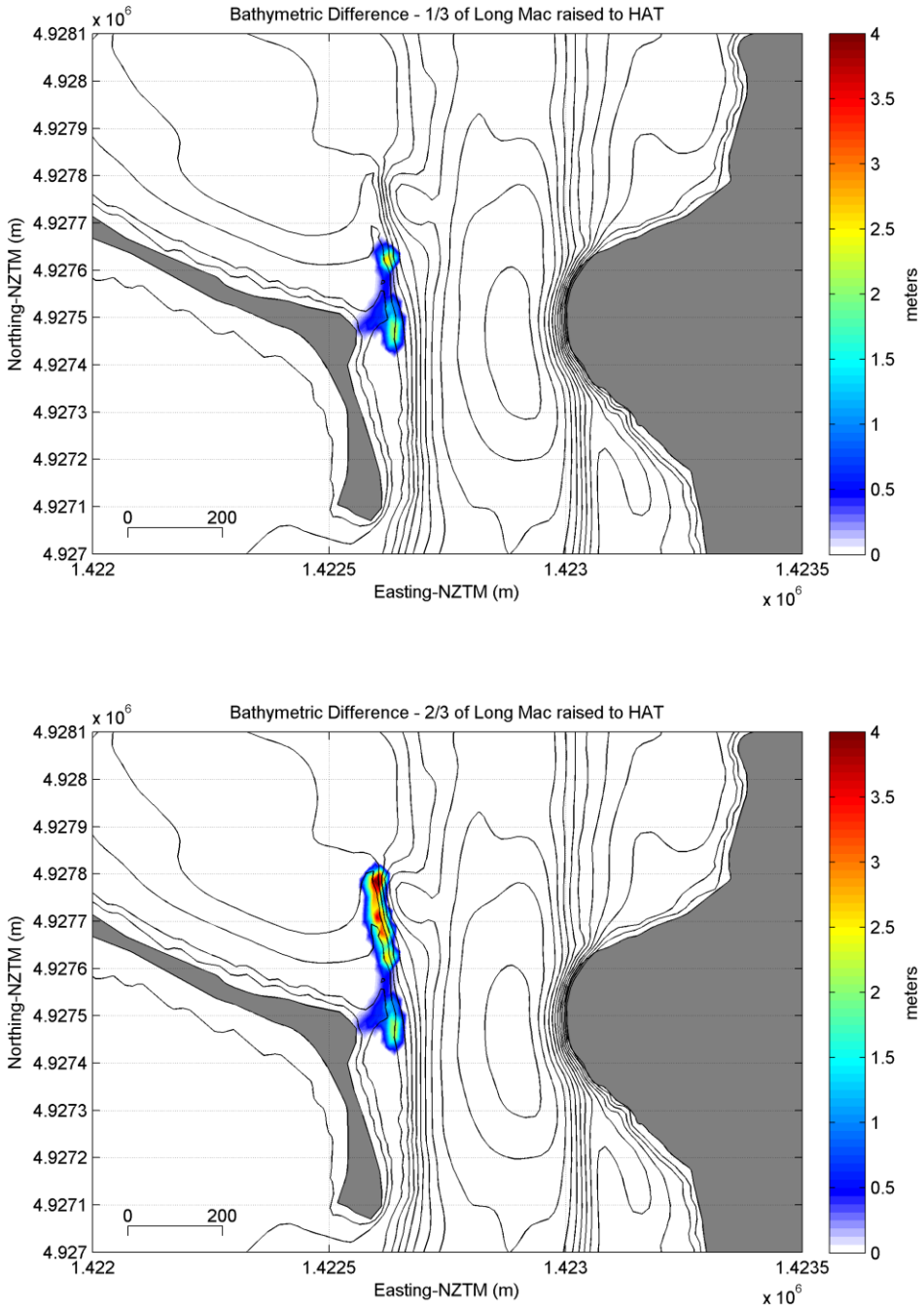

Figure 4.3 Bed level difference between existing and modified model bathymetries (central segment raised to HAT, top, central and north segments raised to HAT, bottom). Note that the bed level at the junction from the eastern tip of Shelly Beach (spit bend) to the structure was also raised so that the beach cell enclosed.